Quasicontinuum variants of diffusion-limited aggregation

Yacov Kantor,* T. A. Witten, and Robin C. Ball†
Corporate Research Science Laboratories, Exxon Research and Engineering Company, Route 22 East, Annandale, New Jersey 08801
(Received 2 December 1985)

Two diffusive-growth models with an indefinite range of local densities are studied, and their fractal scaling properties are compared with those of diffusion-limited aggregation (DLA). The first model, "penetrable DLA," differs from standard DLA in that each diffusing particle interacts arbitrarily weakly with an aggregated particle. We derive an analytic expression for the growth rates and find by simulation that the weak interaction leaves the DLA scaling properties unmodified. We explain the observed dependence of the density on the interaction strength. Our second model is a stochastic differential equation, without discrete particles. Simulations of this equation show fractal scaling properties consistent with those of DLA. The scaling of this model shows new subtleties; the average density and the spatial correlations are controlled by different exponents. We describe the reasons for this novel behavior.

I. INTRODUCTION

The irreversible aggregation of small particles has recently received considerable attention. Several years ago Witten and Sander[1] suggested a simple model of irreversible growth—diffusion-limited aggregation (DLA). In this model a seed aggregate is placed at a lattice site and diffusing particles stick to it and join it if they visit a neighboring site. (A more accurate definition is given in Sec. II.) It has been found[1–3] that such aggregates exhibit some of the striking scale-invariant properties of a fractal[4] object; the complex spatial correlations seen in a piece of the aggregate are reproduced in its subpieces. Such scale invariance implies power-law behavior, e.g., for the average density at distance r from an arbitrary point on the object. For r smaller than the size of aggregate this density goes as r^{D-d}, where D is called the fractal[4] (Hausdorff) dimension and d is the dimension of space. The numerical value of D seen in DLA does not depend on the lattice type, and remains the same also in nonlattice simulations.[5] This power-law behavior occurs in all spatial dimensions where it has been studied; between two and six dimensions D varies smoothly from about $d-\frac{1}{3}$ to about $d-1$.[6(a)] In this study we seek a deeper understanding of this scaling behavior.

The apparent analogy between the aggregation process and the critical phenomena[6(b)] in thermodynamics has led to several theoretical attempts[7,8] to treat the phenomenon similarly to the renormalization-group approach. Various authors have produced approximate expressions for D, which were reasonably close to the known numerical values. But a systematic approximation scheme similar to the renormalized perturbation theories[6(b)] for critical exponents has not been found.

The complex structure of DLA is the more intriguing because of its relationship to other growth phenomena. Growth of a surface by the absorption of a diffusing substance is the mechanism of dendritic crystal growth.[9] This deterministic growth process has long been known to be unstable.[10] Any small irregularities in the initial surface are amplified. The instability leads[11] to the rich, regular patterns. Recently, it has been discovered[12] that the long-range correlations of a diffusing field are not essential in producing these patterns.

In other recently studied cases of diffusive growth, disordered, scale-invariant structures like DLA have been reported. The electrodeposition experiments of Brady and Ball[13] and Matsushita *et al.*[14] reported a fractal dimension D in agreement with that of DLA simulations. The recent viscous fingering experiment of Nittman *et al.*[15] produces branched structures which are virtually indistinguishable from DLA. These systems are like DLA in that the growth at a point is proportional to the flux of a diffusing field onto that point.[16] DLA with a screened diffusing field ceases to show fractal scale invariance at distances larger than the correlation length of that field.[17] The long-range correlations of this diffusing field are evidently essential in producing these structures. But the discrete, stochastic feature of DLA appears inessential, since this feature is not shared by the fingering or electrodeposition experiments.

Since DLA is scale invariant, the statistical correlations measured on some length scale r do not reveal the scale of the microscopic process producing the growth. Thus these details must be irrelevant for determining the future growth at scales r and larger. Only some coarse-grained information, such as the local density averaged over distances smaller than r, should suffice.

These ideas have led us to study DLA-like models in which the microscopic features have been modified or removed, while the growth from a diffusing field has been retained. the simplest of these was the "continuum approximation,"[7] which describes deterministic growth of a smooth density profile from a diffusing field. This solvable model has a suggestive power-law relationship between the density and the size of the profile. It also shows a wrinkling instability like that of dendritic growth.[11] But it does not show the scale-invariant interior correlations of

a fractal object.

In this study we consider two variants of DLA. The first, which we call penetrable DLA, explores the effect of taking the stochastic unit of growth to zero. This leads to a process in which the microscopic randomness is reduced, and in which the local density takes on nearly a continuum of values. In this sense, the model approaches the continuum approximation. Yet, the structure at all length scales shows the scaling behavior of DLA, and nowhere that of the continuum model. We give arguments to account for this apparent paradox. Our second model is a modification of the continuum model to make it more like DLA. We allow the growth at a point to be influenced not only by the continuum equations, but also by random noise. The results depend on the nature of the noise. In the case of "binary noise" (defined below) the DLA structure emerges. In the case of "uniform noise" some scaling properties of the noiseless continuum model are preserved, but the two-point correlation function shows the fractal behavior of DLA. The structure shows scaling features unlike either a smooth density profile or an ordinary fractal object. We discuss how this novel behavior arises.

II. EQUATIONS OF GROWTH

In this section we present a detailed derivation of the equations of the DLA growth we will simulate. The main points of this derivation are not new[3,7] and have been briefly presented by several authors.

Usually DLA is defined in terms of a Monte Carlo procedure. We shall present a somewhat generalized version of DLA which contains the original definition of DLA (Ref. 1) as a limiting case. We start with a single seed particle at the origin of a lattice; this is our initial cluster. An additional particle is launched from a remote point and undergoes a random walk. If it escapes to infinity, an additional particle is launched. If it arrives next to the cluster it can stick to it. The probability $P(x)$ of sticking to a certain point x is given by the number of cluster particles present at the nearest-neighbor sites multiplied by a "sticking parameter" p, plus the number of cluster particles present at the site multiplied by another parameter q (if this sum exceeds unity we assume $P=1$). After a particle has been added to the cluster by this process, a new random walker is released and the process if repeated. Thus P can be conveniently expressed in the following form:

$$P(x)=F((pZ+q)\rho+a^2p\nabla'^2\rho)\ , \tag{1}$$

where ρ is the density (number of particles per lattice site) of the DLA cluster, a and Z are the lattice constant and the coordination number, respectively. The symbol ∇'^2 represents the discrete Laplacian, i.e., the following sum over nearest neighbors $\mathbf{r}+\mathbf{l}$ of a point $\mathbf{r}$: $\sum_{\mathbf{l}\,(\mathrm{nn})}[\rho(\mathbf{r}+\mathbf{l})-\rho(\mathbf{r})]/a^2$. The cutoff function $F(x)$ is defined as $\min(x,1)$. For $p=1$ this represents the standard DLA in which a particle sticks with certainty to a site adjacent to the cluster. (In this case $\rho=0$ or 1 and the random walker can never step on an already occupied site; thus the value of q is irrelevant.) For $p<1$, ρ can assume any integer value between 0 and $1/p$.

The probability that the current walker is added at a site x can be expressed in terms of the probability $\tilde{u}_i(x)$ to find a random walker at the point x on its ith step. In the simulation each step consists of two substeps. First, the walker moves to a randomly chosen adjacent site. The probability that it is then at x is the sum of the probabilities that it was on one of the adjacent sites on the last step, times the probability Z^{-1} that the walker stepped to x. The change $\Delta_1\tilde{u}$ from this substep is simply $Z^{-1}a^2\nabla'^2\tilde{u}$. The second substep is absorption; a walker at x is removed with probability $P(x)$. The resulting change $\Delta_2\tilde{u}$ is $-P(x)(\tilde{u}+\Delta_1\tilde{u})$. The net change over the time step is thus

$$\Delta\tilde{u}=\tilde{u}_{i+1}-\tilde{u}_i=\Delta_1\tilde{u}+\Delta_2\tilde{u}=Z^{-1}a^2(1-P)\nabla'^2\tilde{u}-P\tilde{u}\ . \tag{2}$$

From $\tilde{u}$ we may find the expectation value $u(x)=\sum_{i=0}^{\infty}\tilde{u}_i$ of the number of times site x is visited by a walker. The equation for u is the sum on i of Eq. (2). On the left-hand side we obtain the difference of $\tilde{u}(x)$ between $i=0$ and ∞. Both these terms vanish everywhere except in the distant region where the particles are released. Except for this region the resulting equation reads

$$0=Z^{-1}a^2(1-P)\nabla'^2u-Pu\ , \tag{3}$$

where $P(x)=F((q+pZ)\rho+pa^2\nabla'^2\rho)$, as discussed above. Note that the argument of F is non-negative for $q\geq 0$. The parameter q regulates the relative stickiness of occupied points versus the stickiness of the points adjacent to occupied points. It regulates the speed of the advancing growth front. In all subsequent calculations we shall assume $q=0$. The cutoff function F becomes unimportant if the sticking parameter p is made small. We find below that for $p<1/10Z$, the sticking probability P and hence the argument of F are virtually always less than 1. Thus $F(x)$ can be simply replaced by x. If in addition $P\ll 1$, Eq. (3) simplifies to

$$\nabla'^2u=Za^{-2}p(Z\rho+a^2\nabla'^2\rho)u\ . \tag{4}$$

The average growth at a certain point is proportional to the absorption rate of the diffusing particles. The absorption probability at a site x is the average number of visits to that site times the probability P of absorption per visit. The probability of a visit on the ith time step is $\tilde{u}_i+\Delta_1\tilde{u}_i$. The total number of visits for all time steps is $u+Z^{-1}a^2\nabla'^2u$, where we have used the expression for Δ_1 above Eq. (3). Thus the absorption probability $Q(x)$ is given by

$$Q(x)=P(u+Z^{-1}\nabla'^2u)=Z^{-1}\nabla'^2u\ . \tag{5}$$

The last equality was obtained using Eq. (3), and it means that the amount of growth of a site is equal to the net flux onto it. Since $\sum_x Q(x)=1$, ∇'^2u must obey a normalization condition. Equivalently, the normal derivative of u on the outer spherical boundary must be equal to the inverse surface area of the sphere. Note that this equation gives exactly the average growth rate for given configuration $\rho(x)$, i.e., $Q(x)=(\partial\rho/\partial M)_{\mathrm{av}}$, where the average is

over possible walks of the Mth particle. Equations (4) and (5) can be used as an alternative method of construction of DLA. For each time step the actual change of ρ at any point is found by choosing a site x with probability $Q(x)$ and adding a particle there.

Viewed in this way, the prescription for DLA has two parts: a deterministic part and a stochastic part. The deterministic part, given by Eqs. (4) and (5), prescribes, for a given density profile $\rho(r)$, the probability of growth at any site. The stochastic or random part, described after Eq. (5), directs us to make a change of ρ at a point in accord with these probabilities. The present study investigates various limits in which the amount of randomness is made small.

The growth equations (4) and (5) make sense with the randomness removed altogether. That is, one may simply make the density ρ change by exactly the amount $Q(x)$ given in Eq. (5). This is the "continuum approximation" introduced by Ball, Nauenberg, and Witten,[7] as discussed above. Since this approximation amounts to the replacement of a stochastic quantity by its average, it is a type of mean-field approximation. In it the density ρ is no longer discrete, but may take on a continuum of positive values, which may be arbitrarily small.

The ρ field of the mean-field approximation itself is not a fractal object: In a fractal the decrease of the average density with an increasing length scale is due to appearance of increasingly larger holes, while the typical density of the occupied regions does not depend on the size of the object. A convenient quantitative measure of the typical density is $\langle\rho^2\rangle/\langle\rho\rangle$. Here the average $\langle\cdots\rangle$ is taken over all points of the density profile. This typical density may be expressed in terms of the two-point correlation function $C(r)$. This $C(r)$ is defined by $\langle\rho(0)\rho(r)\rangle/\langle\rho(0)\rangle$, where the averages are taken over all positions and orientations of the density profile with respect to the origin 0. Thus $C(r)$ is the average density at distance r from an arbitrary origin point, where the origin points are weighted in proportion to their density. Evidently, the typical density $\langle\rho^2\rangle/\langle\rho\rangle$ is simply $C(r=0)$.

If ρ can assume only the values 0 and a, then $\langle\rho^2\rangle/\langle\rho\rangle=a$, regardless of the size of the aggregate. A similar result will be obtained if the nonzero values of ρ have a narrow distribution around a. (In general, if the average value of ρ and its variance on a nonempty site are a and V, respectively, then $\langle\rho^2\rangle/\langle\rho\rangle=a+V/a$.) For a smooth density profile, by contrast, $C(0)$ is of the order of the average density $\langle\rho\rangle\sim M/R^d$. Here $C(0)$ does not remain constant, but decreases indefinitely with $\langle\rho\rangle$. Thus $C(0)$ distinguishes a fractal density profile from a generic profile of low average density.

We recall for future reference some qualitative features of the mean-field approximation.[7] The growing profile consists of three regions: an outer, a middle, and an inner one. In the outer region the density has not grown sufficiently to perturb the diffusing field appreciably; thus u is qualitatively a constant. In this region the growth equation (5) simplifies to

$$\frac{\partial\rho}{\partial t}=B(\rho+a^2\nabla'^2\rho)\ . \tag{6}$$

The growth in the outer region eventually reaches sufficient density to cause appreciable reduction of u. The "opaque radius" R_0 where this first occurs increases linearly in time (up to logarithmic modifications). The bulk of the absorption occurs in the "growth region," at distances of the order of R_0. This is the middle region. Inside this is the inner region, where the diffusing field is exponentially small, and the growth is negligible. For the profile as a whole the rate dM/dt of deposition is that of a perfect absorber with radius of the order the opaque radius R_0 defined above. The change in radius with deposited mass M may be inferred from dR/dt and dM/dt. In two dimensions one finds that M grows linearly with R.

This reasoning does not apply to standard DLA, since this has no outer, transparently growing region. The density at a site cannot be indefinitely small; if it is less than one particle, it must be zero. Thus at sufficiently large distances, there is no growth. In contrast, the mean-field density at large distances is exponentially small, but there is still growth—enough growth to affect the screening of the diffusing field and the deposition of mass. The transparent growth region is an unphysical feature of the mean-field model, since it allows indefinitely small densities, while real growth processes have some minimal density below in which no growth occurs.

III. PENETRABLE DLA

In this section we describe the behavior of DLA with small sticking parameter[18] p. We used standard Monte Carlo methods[3] to generate two-dimensional DLA clusters on a square lattice with sticking probabilities $p=1.0$, 0.03, 0.003, and 0.0003 and measured their properties. The masses of these aggregates (3000, 6000, 60 000, and 500 000, respectively) have been chosen to maintain the radius of the circumscribing circle at approximately 100. Figures 1 and 2 depict DLA's with two different sticking probabilities. It can be clearly seen that the decrease of p smooths the density profile and creates wider branches. However, the main properties of the structure do not seem to change. It can be clearly seen from Fig. 2 that the resulting aggregate has a certain typical density which creates a structure similar to the standard DLA depicted in Fig. 1. Furthermore, the apparent smoothing of the profile does not seem to have a large influence on the two-point correlation function $C(r)$. The function $C(r)$ for four different p's is depicted in Fig. 3(a). For r greater than three lattice constants all the functions exhibit a well-defined linear behavior (on the log-log scale) for more than one decade followed by a sharp decrease of $C(r)$ when r becomes of the size of the aggregate. Linear parts of all the curves have the same slope (within the error bars) corresponding to the codimension $d-D\cong 0.3$, which is in good agreement with the known numerical results[5] for a two-dimensional DLA. There are some differences between the curves in the region $1\le r\le 3$: the initial drop observed in the $p=1$ curve disappears in the curves with smaller p and they become more horizontal when p decreases. The range of those differences is too small to be attributed to the appearance of a different power-law

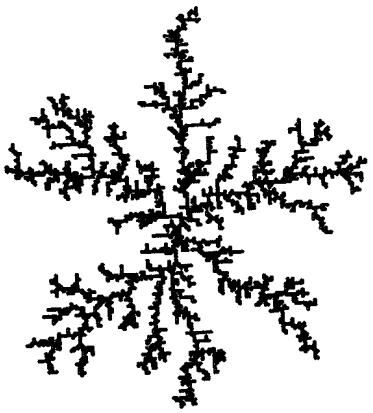

FIG. 1. DLA of 3000 particles generated with sticking probability $p=1$.

regime in $C(r)$; instead, the changes indicate the appearance of a smoothly varying behavior of the density at short-distance scales.

It is interesting to notice that for small p the typical densities $C(0)$ are considerably smaller than the maximal possible value $1/p$. In these four examples the typical densities are 1, 3.6, 12, and 59, while the maximal possible values are 1, 34, 334, and 3334, respectively. We found that for this aggregate $Zp\rho<0.2$ everywhere, and therefore dropping of the cutoff function F in Eq. (4) is certainly justified.

We can understand the way in which the aggregate selects the typical density from the following considerations. Let us consider the initial stages of the growth of an aggregate with an extremely small p. When the mass of the aggregate is still very small, the probability that a random walker approaching the aggregate will be absorbed is also very small, and therefore the particles deep inside and on the exterior of the aggregate are equally well accessible. In the limit $p\to 0$ we can replace our Monte Carlo process with random walkers by a process resembling the Eden model.[19] In this process,[3] which is called the transparent Eden model, a point of a cluster is selected randomly (each point has the same probability to be selected independently of its location) and then the decision whether the particle sticks is made in the same manner as in DLA. This process is described by Eq. (5) in which u is no longer determined by Eq. (4) but is constant. The mean-field approximation of this process is given by Eq. (6). This equation can be readily solved. The density ρ has a Gaussian shape, while the total mass M grows exponentially with time. The actual density profile created by the Monte Carlo process deviates from the prediction of the deterministic Eq. (6); however, it can be

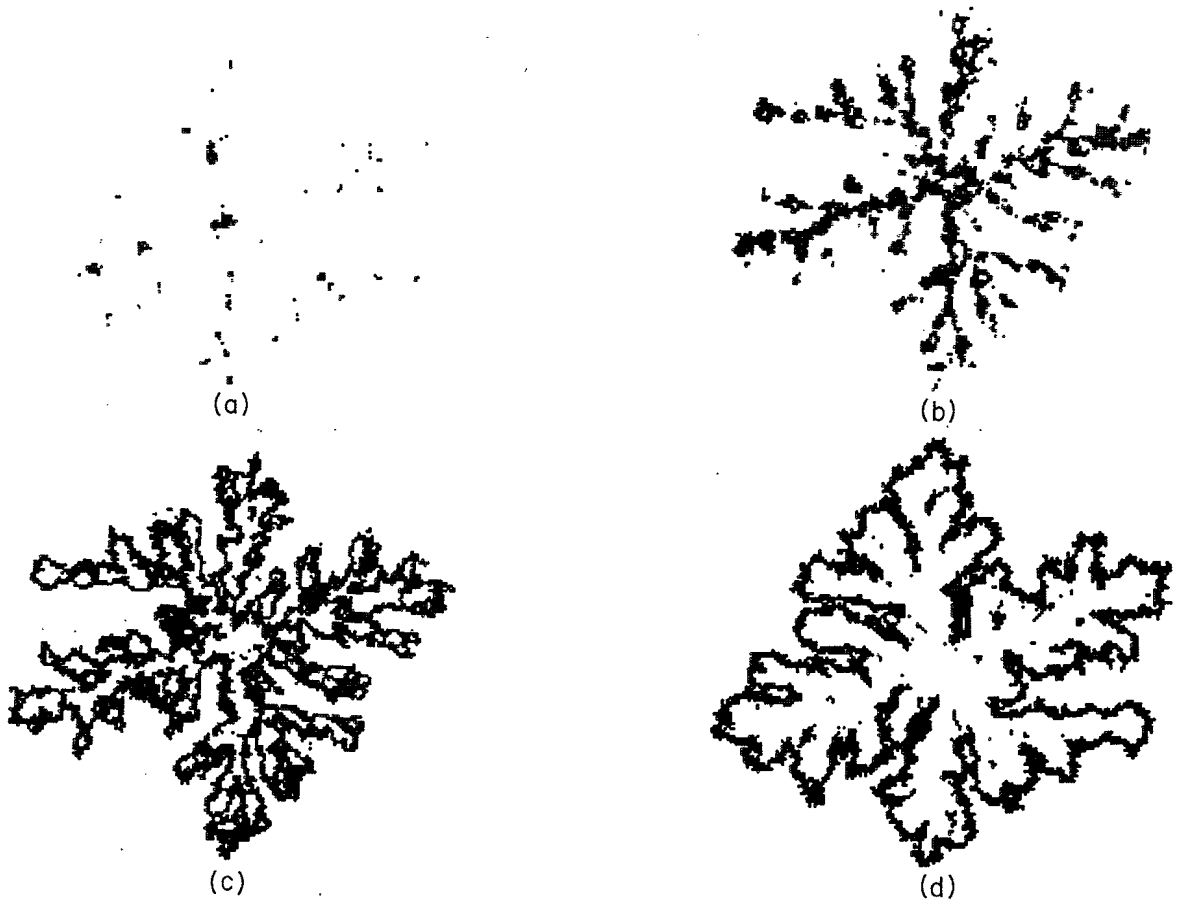

FIG. 2. DLA of 500 000 particles with sticking probability $p=0.0003$. Each figure shows the location of site occupied by a number of particles in a certain range: (a) 120—169, (b) 70—119, (c) 30—69, (d) 1—29.

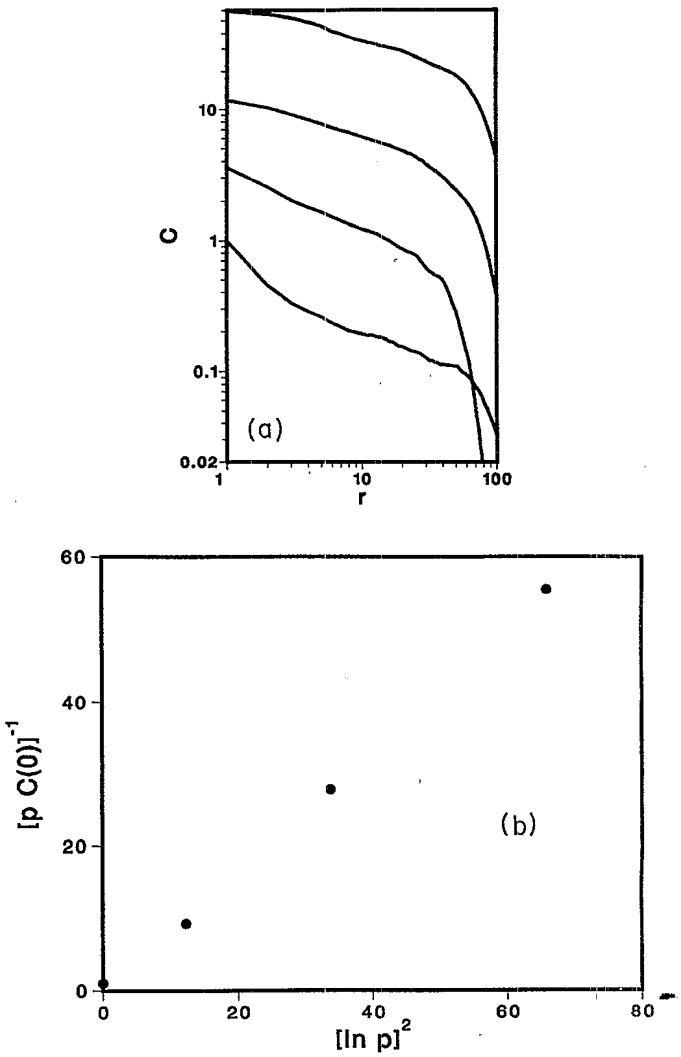

FIG. 3. Correlation functions $C(r)$ for penetrable DLA. (a) Double logarithmic plot showing the dependence on r of the two-point correlation function $C(r)$ of 3000-particle DLA cluster with sticking probability $p=1$ (bottom curve), 6000-particle cluster with $p=0.03$ (second from the bottom), 60 000-particle cluster with $p=0.003$ (third from the bottom), and 500 000-particle cluster with $p=0.0003$ (top curve). (Since we are considering a discrete lattice, $r=n$ means the average in the region $n-1\leq r<n$.) (b) plot showing the apparent linear dependence of the quantity $[pC(0)]^{-1}$ on $\log^2 p$, using the data from (a).

shown[3] that the real average density is what one would obtain by integrating the mean-field equations. Thus for $M\gg 1$ the density of the transparent Eden model is given by

$$\rho(r)=M\exp[-r^2/(2a^2\ln M)]/(2\pi\ln M)^{d/2},$$

where we have eliminated the time in terms of total mass.

Using this density, we may estimate the interaction with a random walker. We may approximate the aggregate as a uniform density within some radius R. We take R as the radius where $\rho(R)=1$; i.e., the boundary of the aggregate. Using the expression above for $\rho(r)$, we find $R\sim\ln M$. A random walker within the aggregate requires about R^2 steps to leave it. Its total probability of absorption is thus of order $p\rho R^2$. When this probability becomes of order unity, the transparent Eden model no longer approximates the DLA; the center becomes screened and stops growing. Using $\rho\sim M/R^{d/2}$, we find that $pM=$const in two dimensions. Thus screening becomes important for $(p\rho)^{-1}\cong R^2\cong-\ln^2 p$.

It is reasonable to assume that the "building blocks" of the aggregate will have this density, so that $[pC(0)]^{-1}\sim\ln^2 p$. Our simulations confirm this dependence, as Fig. 3(b) shows.

We note that the maximal sticking probability at a time step is $Zp\rho_{\max}\sim pC(0)\sim(\log p)^{-2}$. This accounts for our observation that perfectly absorbing sites, where $Zp\rho>1$, become negligible for small p. The changes in the behavior of the correlation function $C(r)$ with decreasing p in Fig. 3 are consistent with the appearance of the transparent Eden modellike behavior for small r. The $C(r)$ should be constant out to distances r of order $\log p$, and then should fall off as in DLA. The observed flattening of $C(r)$ for small r in Fig. 3(a) is in accord with this prediction.

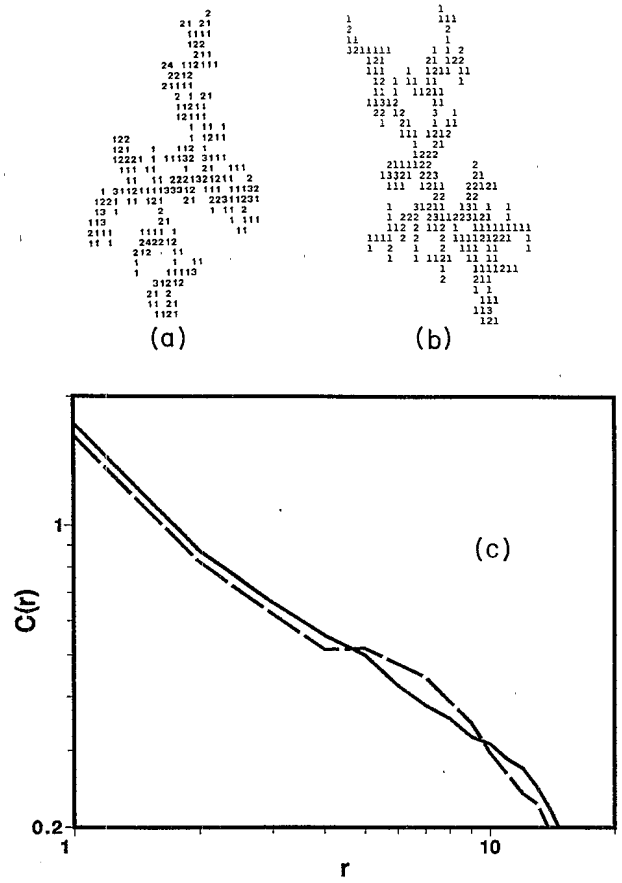

FIG. 4. (a) DLA cluster generated using Eqs. (4) and (5) and using "binary noise" (see text). Numbers denote the number of particles at each site. The total mass (number of particles) is 308. (b) Penetrable DLA cluster with mass 309 and $p=\frac{1}{4}$, produced as described in Sec. III. (c) Correlation function $C(r)$ for cluster in (a) (solid line) and (b) (dashed line).

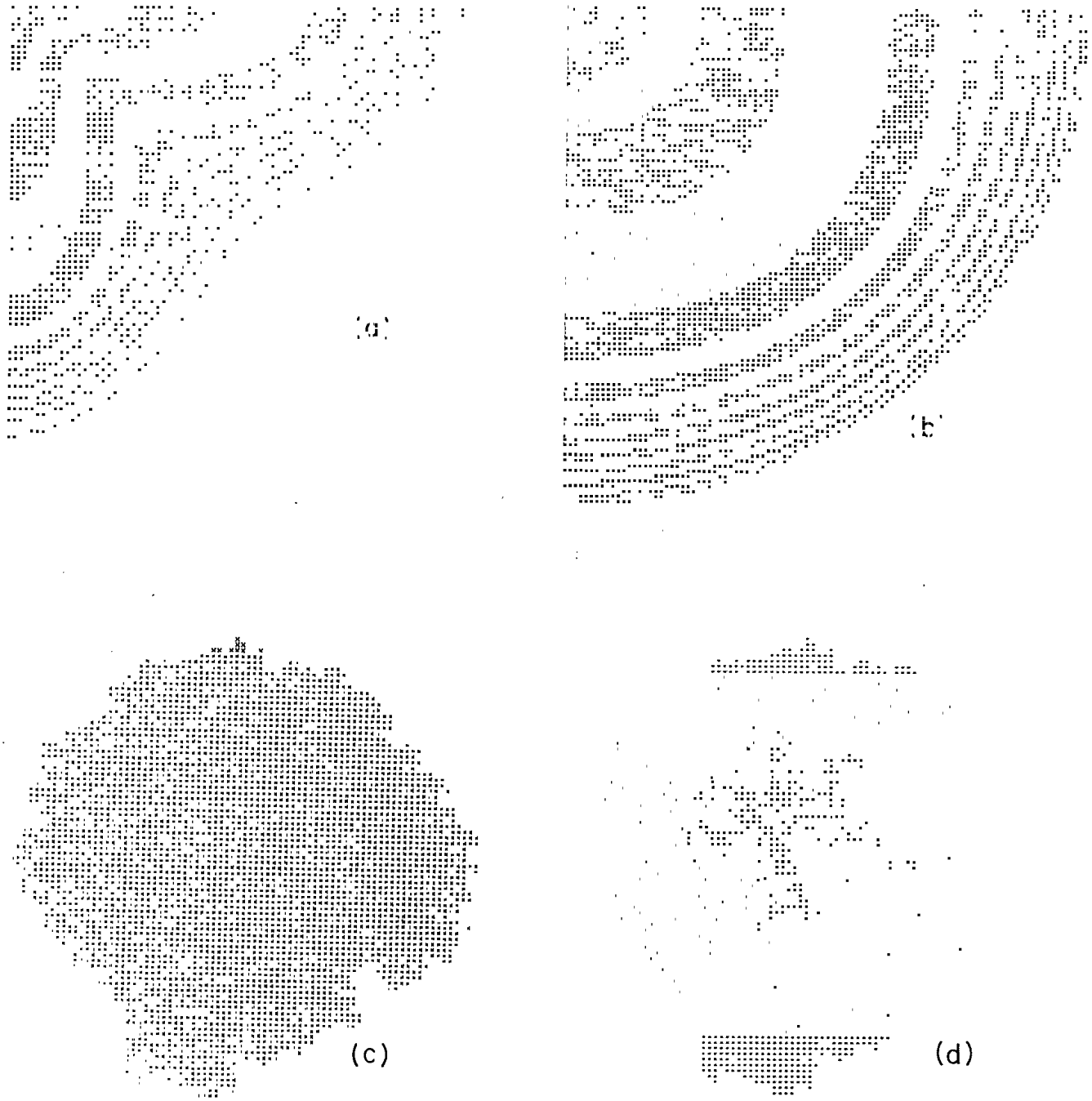

FIG. 5. Density profiles generated by integrating the stochastic growth equations, (4) and (5). (a) Noiseless growth in a single quadrant of the plane. Seed, in upper-left corner, has density about 1.5. Mass for four quadrants is 206; $R_G=30$. Each dark or light band covers a density range of a factor $\sqrt{e}\cong 1.65$. Dashed band has density about equal to the average density $\langle\rho\rangle$ defined in the text. (b) same as (a) except that the average of neighboring densities described below Eq. (1) was replaced by a weighted average of first and second neighbors. The weight for the second neighbors was $\frac{1}{4}$ that of the nearest neighbors. (c) Uniform-noise profile grown as described in the text. Seed was a single site the center with $\rho=1$. The total mass is 35.4, and its radius of gyration is 14.8. Sites where density exceeds 1.5×10^{-8} are shaded. (d) Same as (c), but with only sites with density greater than 0.02 shaded (e). A *uniform*-noise profile grown under the same conditions as (c),(d), but in a single quadrant of space with plus-shaped seed, as described in the text. Mass is 274; $R_G=38$. Sites with density greater than 8×10^{-7} are shaded. (f) Same as (e) but only points with density exceeding 0.02 are shaded.

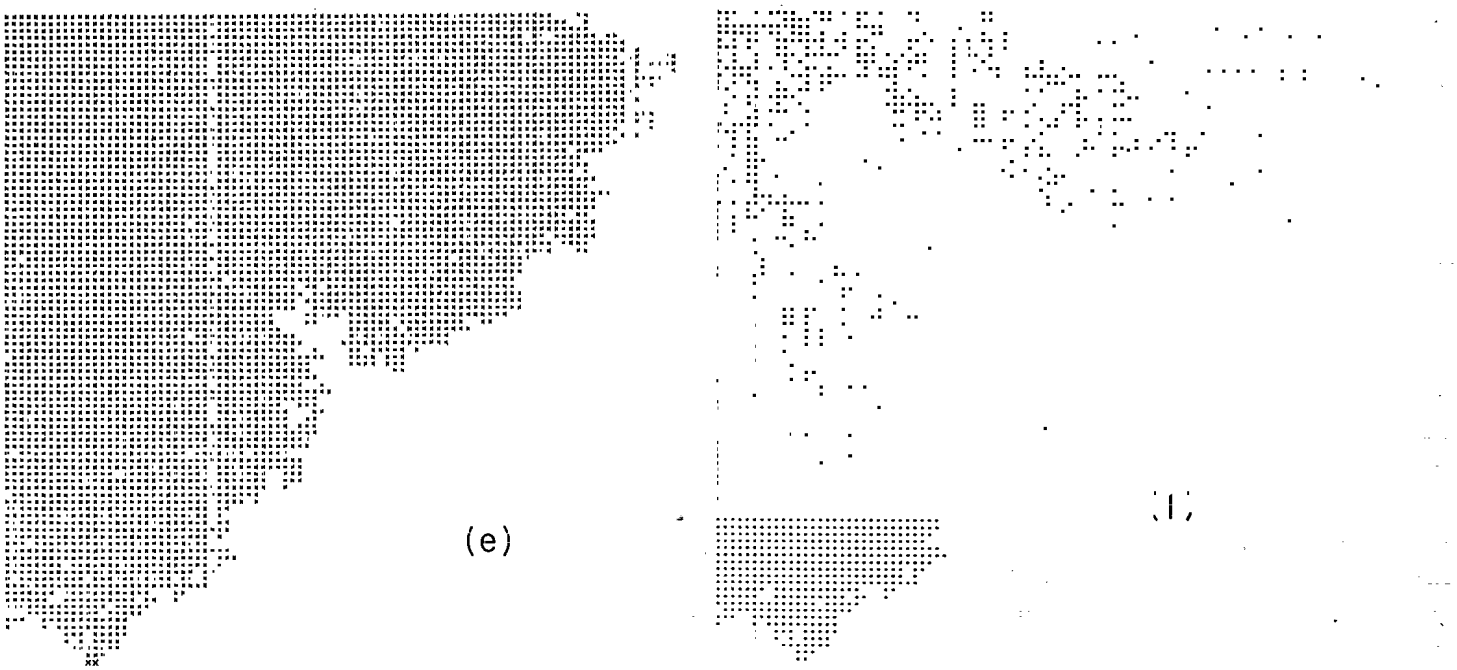

FIG. 5. (*Continued*).

IV. GROWTH FROM THE STOCHASTIC CONTINUUM EQUATIONS

The penetrable DLA studies of Sec. III show that many features of standard DLA may be modified without changing the ultimate scaling behavior. The geometric impenetrability of the cluster is not important and the density at a site may vary almost continuously. Thus the microscopic randomness of the process may be modified drastically without substantial effects. In this section we consider models in which this randomness is modified more radically. In these models there are no random walkers and no aggregating particles. Instead, we consider various implementations of the stochastic growth equations (4) and (5) without restricting the fluctuations as described after Eq. (5). In these simulations the u field of Eq. (4) is found numerically, and a small increment of the density ρ is generated randomly on every site, respecting the average in Eq. (5).

Our main simulation is motivated by the hypothesis that the mere qualitative presence of noise is sufficient to produce DLA scaling. Accordingly, we used a simple multiplicative noise. The actual growth increment at a site was the average given in Eq. (5) times a random number uniformly distributed between 0 and 2. The noise was independent on each lattice site, as it is in actual DLA. This multiplicative uniform noise has a form that assures nonnegative growth at each time step.

As a control we replaced the uniform noise by a noise whose values were only zero or one, weighted so as to have the proper average on each site. This is the prescription for DLA described following Eq. (5). We denote this model as "binary noise."

This control simulation [Fig. 4(a)] produced a cluster indistinguishable from an actual DLA cluster using the same sticking probability p [Fig. 4(b)]. The qualitative appearance was the same as shown in Fig. 4(a), and the correlation functions agreed in both amplitude and r dependence [Fig. 4(b)] as well as one would expect from two DLA clusters of this size. This serves as a check on the simulation program as well as on the reasoning leading to Eq. (5).

For the uniform noise case as well as the above case the simulations were done on a 100×100 square lattice in two dimensions. The seed cluster was a small "plus" sign; i.e., a density of 1.5 at the middle site of this lattice, and a density of 1 on its nearest neighbors. A sticking parameter p of $\frac{1}{4}$ was chosen. The time steps were chosen to assure only a small change in the deposit per time step. In most of the simulations the total mass deposited per time step was regulated to be about unity throughout the growth. Factor-of-2 changes in the time step made no substantial difference in the behavior reported below.[20] The diffusing field u was fixed at 1 on a circle inscribed in the 100×100 lattice. The u field of Eq. (4) was found iteratively using the method of overrelaxation.[21] The iteration was repeated until the sum over the lattice of squares of corrections $(\Delta u)^2$ was smaller than 10^{-5}. Fifty to one hundred iterations were usually required to attain convergence to this tolerance. An order-of-magnitude reduction in the tolerance made only barely perceptible changes in the growth.

To extend the range of growth we supplemented these simulations with "single-quadrant" simulations. Here the noise pattern was taken to have symmetries such that the growth was forced to remain symmetric under reflection in the x or y axes. In practice this allows one to restrict the solution to one quadrant of the lattice. The seed is put in one corner of this quadrant. The u field is forced to be even under reflection in either axis. The single-quadrant scheme was checked by generating a growth increment with a given (reflection-symmetric) density profile and

verifying that the growth at each site was identical to that in the original simulation.

In the uniform noise simulations the effective amount of noise depends on the size of a time step. If the time step is very small, so that the growth of a site occurs over many time steps, then this growth reflects on average of many independent noise values at the various time steps. In effect the amount of noise is reduced. To control this effect, we allowed the noise to remain constant in time during the growth of any lattice site. In practice the noise was frozen; it varied in space, but not in time. We expect that holding the noise constant over a finite correlation time sufficient to allow each site to accomplish most of its growth would have produced the same results.

For comparison we made simulations identical to those described above, except with the noise removed. This is the continuum growth model of Ref. 7. The density profile of a noiseless, single quadrant simulation is shown in Fig. 5(a). The profile is represented as an array of printed characters. The seed is in the upper-left corner. Moving outward from this seed, the alternating bands of characters and dots represent ranges of decreasing density. The scale is logarithmic; each band covers a factor $1.65=\sqrt{e}$ change in density. The band shown as dashes corresponds to the average density 0.07. Evidently, most of the picture contains quite small density. Half of the total mass lies within the solid band beyond the dashed band. The dotted band beyond this contains the most total mass of any single band. This band also occupies the most space in the picture.

The picture shows an obvious breaking of circular symmetry; fingers have developed along the x and y axes. The origin of this is lattice anisotropy.[12,22–24] The lattice enters our growth equations through the discrete Laplacian $\nabla'^2\rho$ in Eq. (4). We report elsewhere[25(a)] our investigation of this lattice effect. It may be suppressed by replacing $\nabla'^2\rho$ by a more isotropic finite difference, as shown in Fig. 5(b). The lattice effect proves unimportant for the simulations with noise reported below. Thus for simplicity we have used ∇'^2 throughout the present study.

In spite of the lattice effect, which leads to increasingly anisotropic fingers within the profile, the outermost region does not show increasing anisotropy. This is the "transparent" region discussed preceding Eq. (6). The diffusing field u becomes irrelevant for this region. Completely transparent growth is not expected to show the lattice instability.[25(b)] Since this outer region controls the density, as discussed below Eq. (6), we expect this density to vary as described there: as the inverse distance from the origin.

The uniform-noise profiles shown in Figs. 5(c)—5(f) are clearly different from the noiseless case. In Fig. 5(c) all points with density ρ above about 10^{-8} are shaded. To make the structure apparent we have reprinted the profiles in Fig. 5(d) showing only densities larger than a threshold. This threshold is of the order of the average density and the dark region contains the bulk of the mass. Figures 5(e) and 5(f) show a single-quadrant profile, represented the same way.

The profiles have the appearance of a connected, branched structure, surrounded by a diffuse, low-density cloud or halo. The cloud is apparently an outer, transparent-growth region similar to that in the noiseless profile. The relative homogeneity of the outer region suggests that it is not qualitatively affected by the noise. Thus one might expect that this region grows to opacity in qualitatively the same way as for the noiseless case. In that case the reasoning below Eq. (6) again would apply and the average density $\langle\rho\rangle$ should scale as the inverse radius. The bulk of the structure, shown in Figs. 5(d) and 5(f), is evidently radically affected by the noise. In contrast to the local randomness seen in the outer region, there are now marked long-range spatial correlations. The branches appear to occupy a progressively decreasing proportion of the image, as a fractal structure would. The preferred growth along the x and y axes has disappeared; instead, there are two dominant branches canted inward from the axes.

The graphs in Fig. 6 make a quantitative comparison between the noiseless and noise cases. Figure 6(a) shows the scaling of the average density $\langle\rho\rangle$ with the radius of gyration R_G. The quantity $\langle\rho\rangle R_G$ is plotted against $R_G^{-1/2}$. In isotropic noiseless growth this ratio goes to a constant in the limit of large R_G. The same appears true for the anisotropic noiseless growth. The density decreases to the asymptotic behavior with a leading correction apparently varying roughly as $R_G^{-1/2}$. The product $\langle\rho\rangle R_G$ is also approximately constant for the noise simulations. It fluctuates narrowly in a 5% range as R_G varies over an order of magnitude. As anticipated above, the scaling of the average density is unaffected by either noise or lattice anisotropy.

We compare the correlation functions $C(r)$ for the noiseless and noisy profiles in Fig. 7(a). The $C(r)$ for the smooth, isotropic noiseless growth, calculated as in Ref. 7,

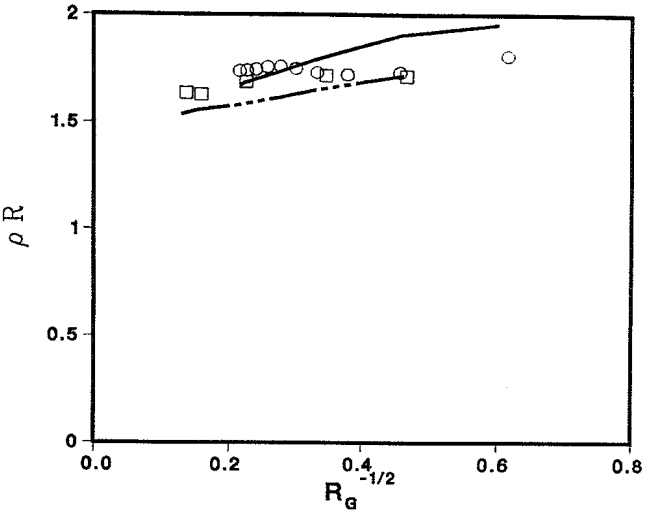

FIG. 6. Evolution of the average density $\langle\rho\rangle$ for stochastic-equation profiles. The quantity $R_G\langle\rho\rangle$ is plotted against $R_G^{-1/2}$. Curves are for noiseless growth: lower curve, single quadrant, cf. Fig. 5(a); upper curve, full plane, profile not shown. The symbols are from uniform-noise simulations. Squares, single quadrant, cf. Figs. 5(e) and 5(f). Circles, full plane, same conditions as Figs. 5(c) and 5(d); profile not shown.

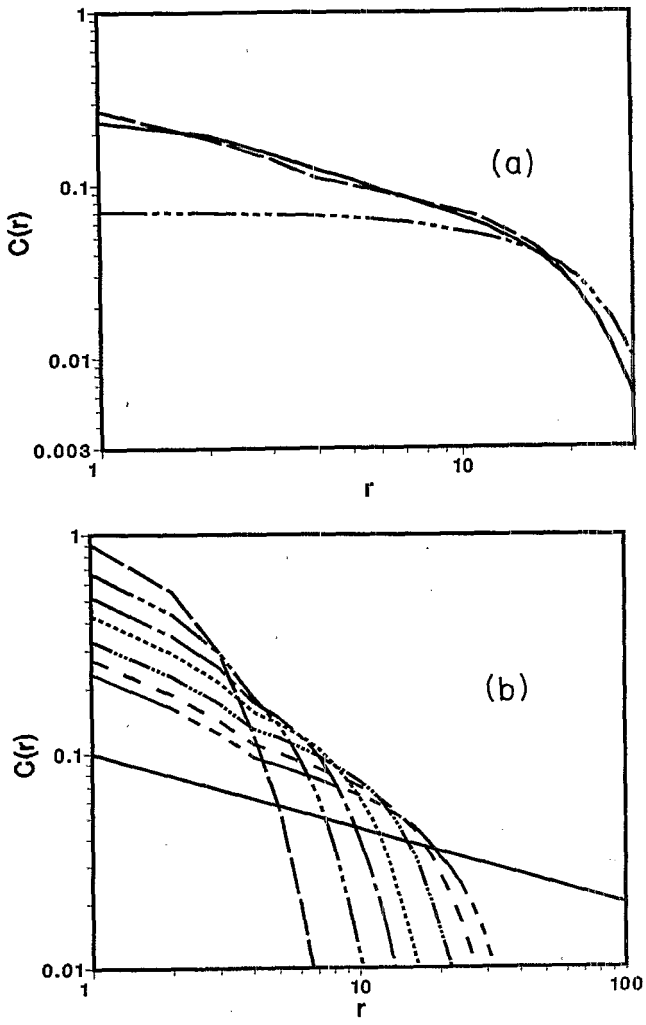

FIG. 7. Correlation functions $C(r)$ for three profiles with mass $\cong 94$. (a) Lower curve, isotropic continuum model; solid curve, anisotropic continuum model of Fig. 5(a); remaining curve, a profile grown under the same conditions as Fig. 5(c) and 5(d) with mass 94.3 and $R_G = 17.2$. (b) Evolution of the correlation function during growth for noisy simulation described in (a). Curves for mass 15, 26, 37, 49, 71, 94, and 117 are shown. The straight line, drawn for reference, has a slope of -0.35.

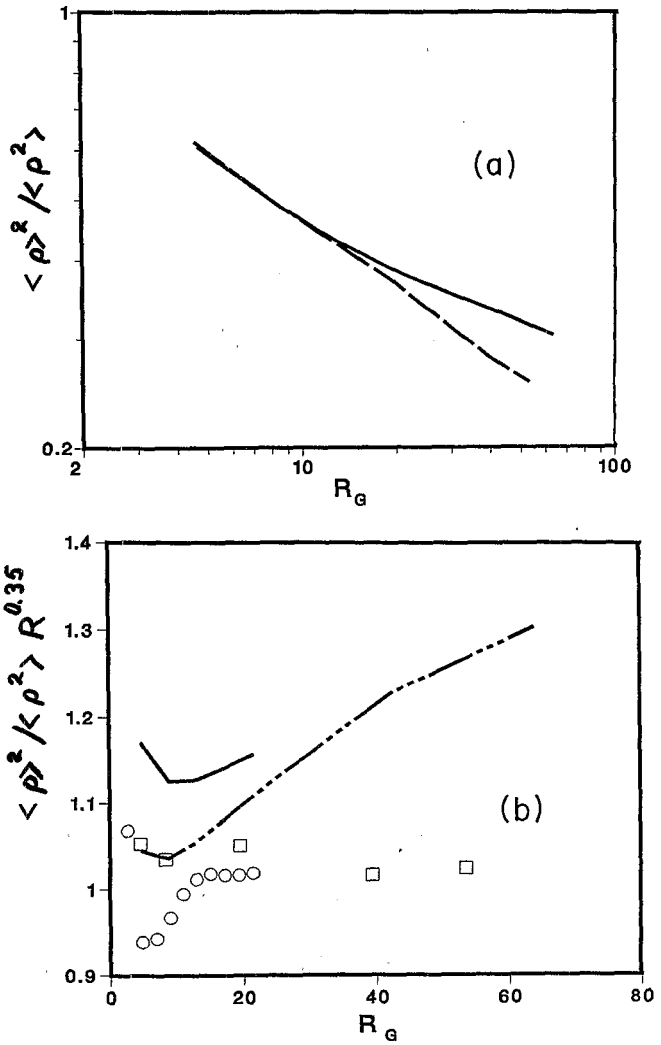

FIG. 8. $\langle \rho \rangle / C(0)$ vs R_G. (a) Upper curve, noiseless, simulation of Fig. 5(a). Lower curve, noisy, simulation of Figs. 5(e) and 5(f). (b) $\langle \rho \rangle^2 / \langle \rho^2 \rangle R_G^{0.35}$ vs R_G. Curves are noiseless simulations; symbols are uniform-noise simulations, as in Fig. 6.

is plotted for comparison. This function shows the regular behavior of a smooth object for $r \ll R_G$. By contrast, the noisy case shows a strong suggestion of a power-law behavior, but shows no clearcut difference from the anisotropic, noiseless case. Figure 7(b) illustrates how the power-law behavior develops during the growth of a profile. The apparent power behavior extends over a progressively longer range, while the apparent power itself remains roughly constant.

To make clear the difference between these profiles and a smooth profile, we have examined the evolution of the typical density $C(r=0) \equiv \langle \rho^2 \rangle / \langle \rho \rangle$ during the growth. For a smooth object $C(0)$ is of the order $\langle \rho \rangle$, as noted above. This is the behavior of the isotropic mean-field solution of Ref. 7 and Fig. 7(a). On the other hand, an irregular, scale-invariant profile, with $C(r) \sim r^{-A}$ for $r \lesssim R_G$, must have $C(0)$ progressively larger than $\langle \rho \rangle$ as R_G increases. For such $C(r)$ we have $\langle \rho \rangle \sim C(R_G)$, so that $C(0)/\langle \rho \rangle \sim R_G^A$. In Fig. 8 we compare $\langle \rho \rangle / C(0) \equiv \langle \rho \rangle^2 / \langle \rho^2 \rangle$ for the noiseless and noisy simulations. Figure 8(a) is a simple log-log plot. The curve for the noisy case is approximately a straight line, suggesting a power law of exponent 0.35. The noiseless case, though not greatly different, shows curvature. In Fig. 8(b) we replot the data to emphasize the different behavior of the two cases. The ratio $\langle \rho \rangle^2 / \langle \rho^2 \rangle R_G^{0.35}$ is plotted versus R_G. The curves 1 and 2 for the two noisy simulations both suggest that this ratio attains a finite asymptote, again consistent with the 0.35-power behavior. Curves 3 and 4 for the noiseless simulations, by contrast, continue to increase. The power behavior seen in these plots confirms that seen in the $C(r)$ plots. The apparent exponent $A \cong 0.35$ is consistent in the two plots, though the power is seen over a wider range in the $C(0)$ plots of Fig. 8.

V. DISCUSSION

The uniform noise simulation appears to show an intermediate scaling behavior not hitherto reported in a growth model. Its overall mass-radius scaling is that of the mean-field or noiseless models. This is natural, since the growth of the mass with size is believed to be controlled by the outer, transparent region.[7,11] In this region the instability associated with *diffusive* growth is absent, and the cooperative effects of noise should be correspondingly not decisive. The lack of correlated structure in the outer region is seen qualitatively in the simulations as well.

Even though the total mass is forced to grow as in the noiseless case, the distribution of this mass in space inside the outer transparent region is still free to show the instabilities of diffusive growth. In other known cases, these instabilities lead to the $r^{-0.3}$ correlations of DLA. This remained true in our studies with small sticking probability, where the local density takes on a near continuum of values, and when the effect of a single-growth event on the profile is made indefinitely small. It is natural for the same behavior to emerge in the uniform noise case.

The "typical density" $C(0)$ in the uniform-noise model does not behave as in DLA. In DLA $C(0)$ remains constant; the aggregate is made of some characteristic building block which maintains its integrity throughout the growth. In standard DLA this building block is a single particle; with small sticking probability it is the opaque unit of order $(p \log^2 p)^{-1}$. In the uniform-noise model, there is no underlying connected structure with a fixed characteristic density. Thus, in contrast to ordinary fractal structures there is no reason for the typical density $C(0)$ to remain fixed. Indeed, the constraint on the total mass, together with a DLA-like correlation function, dictate that $C(0)$ decrease as the cluster grows. Because of this feature of decreasing $C(0)$, the uniform-noise model represents a new kind of scaling behavior that distinguishes it from other fractal structures in statistical physics, such as random walks, percolation clusters, and other particle and cluster aggregates.

The new scaling behavior suggests a picture of DLA made with branches of a density $C(0)$ which decreases as the profile grows, roughly as $R^{-0.6}$. Since these branches must be strongly screening, they must have a width or thickness h which also grows as the profile grows. To maintain screening within the branch requires $h^2 \gtrsim C(0)^{-1} \sim R^{0.6}$, using the same reasoning used above for penetrable DLA. Using this estimate, the thickness h grows slower than the radius R and becomes negligible compared to R; the profile becomes increasingly irregular and locally inhomogeneous.

VI. CONCLUSION

This exploratory study suggests that the uniform-noise model has DLA scaling as discussed above. But extensive work is needed to establish this reliably. The scaling with noise amplitude must be established and DLA scaling must emerge independent of the amplitude. The obvious extensions to larger lattices, higher dimensions, different sticking coefficients, and different forms of noise should also be made. It may emerge from these studies that the 0.35-power scaling seen here is distinct from that of DLA. The uniform-noise model may even prove to produce a simple structure with no fractional power-law properties. Still, the growth mechanisms of the model, its qualitative appearance, and its measured scaling properties all suggest the behavior of DLA.

The uniform-noise model is essentially a continuum formulation, with no elementary unit of structure, either in the form of discrete particles or of a sharp surface. Being a continuum description, it is in a sense explicitly scale invariant. In this sense it is analogous to Wilson's continuum formulation of continuous phase transitions.[26] In phase transitions, the discovery of a continuum formulation laid the basis for understanding of the scaling properties, as discussed above. An analogous treatment of the growth equations appears promising for explaining DLA scaling as well.

ACKNOWLEDGMENTS

We are grateful to Michael Cates and Schlomo Alexander for enlightening discussions.

*Present address: Physics Department, Harvard University, Cambridge, MA 02138.

†Present and permanent address: Cavendish Laboratory, University of Cambridge, Cambridge CB3 0HE, United Kingdom.

[1]T. A. Witten and L. M. Sander, Phys. Rev. Lett. **47**, 1400 (1981).

[2]S. R. Forrest and T. A. Witten, J. Phys. A **12**, L109 (1979).

[3]T. A. Witten and L. M. Sander, Phys. Rev. B **27**, 5686 (1983).

[4]B. Mandelbrot, *Fractals: Form, Chance, and Dimension* (Freeman, San Francisco, 1977); *The Fractal Geometry of Nature* (Freeman, San Francisco, 1982).

[5]P. Meakin, Phys. Rev. A **27**, 2616 (1983).

[6](a) R. Ball, and T. A. Witten, Phys. Rev. A **29**, 2966 (1984). (b) T. Lubensky and J. Isaacson, *ibid.* **20**, 2130 (1979).

[7]R. Ball, M. Nauenberg, and T. A. Witten, Phys. Rev. A **29**, 2017 (1984).

[8]M. Muthukumar, Phys. Rev. Lett. **50**, 839 (1983); M. Tokuyama and K. Kawasaki, Phys. Lett. **100A**, 337 (1984); H. G. E. Hentschel, Phys. Rev. Lett. **52**, 212 (1984).

[9]J. S. Langer and H. Mueller-Krumbhaar, Acta Metall. **26**, 1081 (1978); **26**, 1689 (1978); **26**, 1697 (1978).

[10]W. W. Mullins and R. F. Sekerka, J. Appl. Phys. **34**, 323 (1963).

[11]M. Nauenberg, L. Sander, Physica (Utrecht) A **123**, 360 (1984).

[12]E. Ben-Jacob, N. Goldenfeld, J. S. Langer, and G. Schon, Phys. Rev. Lett. **51**, 1930 (1983); R. C. Brower, D. A. Kessler, N. Koplik, and H. Levine, Phys. Rev. A **29**, 1335 (1984); Phys. Rev. Lett. **51**, 1111 (1983).

[13]R. M. Brady and R. C. Ball, Nature **309**, 225 (1984).

[14]M. Matsushita, M. Sano, Y. Hayakawa, H. Honjo, and Y. Sawada, Phys. Rev. Lett. **53**, 286 (1984).

[15]J. Nittman, G. Daccord, and H. E. Stanley, Nature **314**, 141

(1984).
[16]T. A. Witten and P. Meakin, Phys. Rev. B **28**, 5632 (1983).
[17]L. Niemeyer, L. Pietronero, and H. J. Wiesmann, Phys. Rev. Lett. **52**, 1103 (1984).
[18]An *im*penetrable DLA model with low sticking probability was treated in Ref. 3.
[19]M. Eden, in *Proceedings of the Fourth Berkeley Symposium of Mathematical Statistics and Probability,* edited by J. Neyman (University of California, Berkeley, 1961), Vol. IV, p. 223.
[20]The overall density of the growth was sensitive to the size of the time step; a decrease of this density by as much as a factor of 2 could be seen by reducing the time step a factor of 8 or more. However, the scaling behavior appeared to be the same as reported here.
[21]D. Young, Trans. Am. Math. Soc. **76**, 92 (1954).
[22]R. M. Brady and R. C. Ball, CECAM Workshop, Orsay France, September 1984 (unpublished); P. Meakin, in *Growth and Form, a Modern View,* edited by N. Ostrowsky and H. E. Stanley (Martinus Nijhoff, The Hague, 1985).
[23]E. Ben-Jacob, R. Godbey, N. D. Goldenfeld, J. Koplik, H. Levine, T. Mueller, and L. M. Sander, Phys. Rev. Lett. **55**, 1315 (1986).
[24]M. E. Glicksman, Mater. Sci. Eng. **65**, 45 (1984).
[25](a) Y. Kantor and T. A. Witten (unpublished). (b) This "penetrable Eden model" is discussed by T. A. Witten, in *On Growth and Form, a Modern View,* Ref. 22.
[26]K. G. Wilson and J. Kogut, Phys. Rep. **12C**, 75 (1974).